

¹²C-rich shell, and the ¹³C that would ameliorate the ¹²C purity and the ¹⁵N excess that is common in supernova particles (7, 9) both lie in O-rich gas. The large overabundance of daughter element ⁴⁴Ca of 60-year radioactive ⁴⁴Ti in some of these supernova particles (9, 10) unequivocally demonstrates their supernova origin (11). Our results liberate the analysis from the problems caused by trying to avoid O-rich gas.

These same principles also enable oxides to grow within supernova gas having C > O. Possible evidence of such an oxide grain has been reported (26) in a corundum (Al₂O₃) grain from the Semarkona meteorite with a large excess of ¹⁸O. This large ¹⁸O excess exists in the He-burning shell of the supernova, which is also the only supernova shell that has C > O (1, 25), a composition that would otherwise be expected under thermochemical equilibrium to prevent condensation of an aluminum oxide solid by locking up the O in CO molecules. The radioactivity in supernovae maintains free ¹⁸O atoms in the C-rich shell. However, because the ¹⁸O excess in this grain is only of a factor of 3.2 (26) (so that its condensation requires admixture of a large amount of ¹⁶O), it cannot be concluded that condensation began in the He-burning shell—only that it utilized gas from that shell. Maintenance of free C and O atoms by radioactivity may enable C grains and oxide grains to condense from the same gas.

References and Notes

1. T. A. Weaver and S. E. Woosley, *Phys. Rep.* **227**, 65 (1993).
2. D. D. Clayton and L.-S. The, *Astrophys. J.* **375**, 221 (1991).
3. W. Liu and A. Dalgarno, *ibid.* **454**, 472 (1995).
4. Preliminary discussions of how radioactivity-dominated chemistry facilitates the growth of C dust have been presented [D. D. Clayton, *Lunar Planet. Sci.* **XXIX**, #1016 CD-ROM (1998); *Meteoritics* **33**, A32 (1998); in *Stellar Evolution, Stellar Explosions, and Galactic Chemical Evolution*, A. Mezzacappa, Ed. (Institute of Physics Publishing, Bristol, UK, 1998), pp. 3–13].
5. C. M. Sharp and G. J. Wasserburg, *Geochim. Cosmochim. Acta* **59**, 1633 (1995); K. Lodders and B. Fegley, *Meteoritics* **30**, 661 (1995); *Astrophys. J.* **484**, L71 (1997); in *Astrophysical Implications of the Laboratory Study of Presolar Materials*, T. Bernatowicz and E. Zinner, Eds. (American Institute of Physics, Woodbury, NY, 1997), pp. 391–424.
6. T. Bernatowicz et al., *Astrophys. J.* **472**, 760 (1996).
7. S. Amari and E. Zinner, in *Astrophysical Implications of the Laboratory Study of Presolar Materials*, T. Bernatowicz and E. Zinner, Eds. (American Institute of Physics, Woodbury, NY, 1997), pp. 287–306.
8. T. Bernatowicz and R. M. Walker, *Phys. Today* **50**, 26 (1997).
9. P. Hoppe, R. Strebler, P. Eberhardt, S. Amari, R. S. Lewis, *Science* **272**, 1314 (1996); L. R. Nittler, S. Amari, E. Zinner, S. E. Woosley, R. S. Lewis, *Astrophys. J.* **462**, L31 (1996).
10. D. D. Clayton, S. Amari, E. Zinner, *Astrophys. Space Sci.* **251**, 355 (1997).
11. D. D. Clayton, *Nature* **257**, 36 (1975).
12. ———, *Moon Planets* **19**, 109 (1978).
13. E. Herbst, H.-H. Lee, D. A. Howe, T. J. Millar, *Mon. Not. R. Astron. Soc.* **268**, 335 (1995); R. P. A. Bettens, H.-H. Lee, E. Herbst, *Astrophys. J.* **443**, 664 (1994); R. P. A. Bettens and E. Herbst, *ibid.* **478**, 585 (1997).

14. R. P. A. Bettens and E. Herbst, *Int. J. Mass Spectrom. Ion Processes* **149/150**, 321 (1995).
15. ———, *Astrophys. J.* **468**, 686 (1996).
16. R. Terzieva and E. Herbst, *ibid.* **501**, 207 (1998).
17. C. M. Andreazza and P. D. Singh, *Mon. Not. R. Astron. Soc.* **287**, 287 (1997).
18. K. F. Freed, T. Oka, H. Suzuki, *Astrophys. J.* **263**, 718 (1982).
19. D. R. Bates, *ibid.* **267**, L121 (1983).
20. E. Herbst and R. C. Dunbar, *Mon. Not. R. Astron. Soc.* **253**, 341 (1991).
21. D. E. Woon and E. Herbst, *Astrophys. J.* **465**, 795 (1996).
22. L. B. Lucy, I. J. Danziger, C. Gouffes, P. Bouchet, in *Structure and Dynamics of the Interstellar Medium*, vol. 120 of *IAU Colloquium Series*, G. Tenorio-Tagle, M. Moles, J. Melnick, Eds. (Springer-Verlag, Berlin, 1989), pp. 164–175.
23. A. Van Orden and R. J. Saykally, *Chem. Rev.* **98**, 2313 (1998).
24. D. D. Clayton and N. C. Wickramasinghe, *Astrophys. Space Sci.* **42**, 463 (1976); D. D. Clayton, *ibid.* **65**, 179 (1979).
25. D. D. Clayton, *Proc. Lunar Planet. Sci. Conf.* **12B**, 1781 (1981).
26. B.-G. Choi, G. R. Huss, G. J. Wasserburg, R. Gallino, *Science* **282**, 1284 (1998).
27. This research was supported by the NASA Cosmochemistry Program (D.D.C.), the Origins of Solar Systems Program (D.D.C.), and the Astrophysics Theory Program (W.L.); by the U.S. Department of Energy under contract DE-AC05-96OR22464 with Lockheed Martin Energy Research Corporation (W.L.), and by NSF Division of Astronomical Sciences (A.D.).

7 October 1998; accepted 25 January 1999

A Semiconductor-Based Photonic Memory Cell

S. Zimmermann,¹ A. Wixforth,^{1*} J. P. Kotthaus,¹ W. Wegscheider,² M. Bichler²

Photonic signals were efficiently stored in a semiconductor-based memory cell. The incident photons were converted to electron-hole pairs that were locally stored in a quantum well that was laterally modulated by a field-effect tunable electrostatic superlattice. At large superlattice potential amplitudes, these pairs were stored for a time that was at least five orders of magnitude longer than their natural lifetime. At an arbitrarily chosen time, they were released in a short and intense flash of incoherent light, which was triggered by flattening the superlattice amplitude.

Storing light for appreciable amounts of time is not an easy task because light is always propagating. In principle, light can only be stored directly by guiding its path in a loop back to the origin [for example, in a cavity in which a light beam is folded back and forth between two mirrors or a whispering gallery-type resonator (1)] or by guiding the light along a coil of optical fiber (2). However, to reach delay times of the order of 1 μs, one must use mirrors that lose very little light to obtain the necessary 300 reflections in a 1-m-long cavity, or equivalently, one must use 300 m of fiber to form the loop. Another recently realized approach to light storage uses Anderson localization (3); for this method, the light path is prolonged by passing it through a nonabsorbing but highly scattering medium. In addition to being bulky, these techniques in general do not allow for easily variable delay times.

For optical signal processing (2) and pattern recognition, however, one would like to store the photonic signals in an array of pixels

that can be implemented on a chip. Analogous to an electronic memory where electrons are stored in a capacitor, each pixel could act as an optical memory for intermediate storage or delay of selected optical bits. Such memory cells are the most important part that is still missing from an optical network unit (2). Ideally, such a device would be a small container in which an incoming optical signal could be stored for an arbitrarily chosen time and then be released again as light. The switching speed should be of the order of 1 gigabit/s for local area network applications. Attempts to develop this device rely on a hybrid solution, in which a “smart pixel” (4) registers the light with a conventional detector, converting it to an electrical signal that is then stored in an electronic memory cell. At a given time, the signal can be reconverted to light by using, for example, a laser diode as an emitter. This approach, however, is a complex solution requiring many different techniques and components for a single pixel.

Here, we report the realization of a conceptually different, yet simple and potentially very efficient, storage cell for optical energy, which is based on a field-effect tunable lateral potential modulation in the plane of a semiconductor quantum well (QW). In such a cell, light energy can be locally accumulated and stored for many microseconds by convert-

¹Sektion Physik und Center for Nanoscience, Ludwig-Maximilians-Universität, Geschwister-Scholl-Platz 1, D-80539 München, Germany. ²Walter-Schottky-Institut, Technische Universität München, Am Coulombwall, D-85748 Garching, Germany.

*To whom correspondence should be addressed. E-mail: achim.wixforth@physik.uni-muenchen.de

ing it into spatially separated electron-hole (e^-h^+) pairs. At a chosen moment, the light can be reemitted from the cell in a short and intense flash. The radiative recombination lifetime of photogenerated e^-h^+ pairs can be voltage-tuned over many orders of magnitude from ~ 1 ns to several tens of microseconds (much longer storage times are anticipated). Analogous to electronic dynamic random access memory (DRAM), an optical DRAM can thus be realized, which we envision to be potentially very attractive for optical pattern recognition and image processing. Deliberate release of the light is achieved by triggering the radiative recombination of the stored charges. Each pixel cell can be very small, and storage and emission are controlled by low-voltage signals. However, the photoluminescence (PL) mechanism exploited for intermediate storage does not conserve the coherence of light.

For optical storage, both large absorption and long storage times are desired. Direct band gap semiconductors have strong absorption above the band gap, but the radiative lifetime of the photogenerated e^-h^+ pairs usually is in the range of nanoseconds (5). In contrast, indirect band gap semiconductors have longer radiative lifetimes, yet the interband absorption is small. We combined strong interband absorption with variable lifetimes that were tailored by a low-voltage-induced lateral electrostatic superlattice. The lifetime of the radiative e^-h^+ recombination in a QW can be tuned by the overlap between the e^- and h^+ wave functions (5). When this

overlap is considerably reduced by spatially separating the photogenerated e^-h^+ pairs, very long lifetimes can be achieved without losing the large absorption of the host material. Radiative recombination of the stored electrons and holes through a fast direct transition can then be triggered at a later arbitrary time by removing the electric potential modulation that is responsible for their spatial separation.

Recently, Rocke *et al.* (6) and Rufenacht *et al.* (7) showed that a spatial separation can be used to prolong the lifetimes of photogenerated electrons and holes in a QW. Rocke *et al.* (6) created a lateral potential modulation with a piezoactive sound wave propagating on the sample surface. At a remote location, radiative recombination of the transported bipolar charges was induced by flattening the potential modulation. Rufenacht *et al.* (7) used the built-in potential of a special coupled double QW and triggered the recombination by optically exciting the electrons into an energy state common to both QWs.

To store photonic signals, we used interdigitated gate electrodes on the surface of a QW heterostructure (Fig. 1A). A voltage dif-

ference that was applied to the gates resulted in a lateral type II potential superlattice with an electrically tunable amplitude in the plane of the QW (Fig. 1B). Upon illumination and for lateral electric field components that are strong enough to prevent the formation of excitons, the photogenerated electrons and holes drifted according to their respective charge along the gradient of the lateral potential into laterally opposite directions and accumulated in their respective potential minima (6). They can be stored in these minima for appreciable amounts of time because the overlap of the e^- and h^+ wave functions is dramatically reduced, and they are confined to the potential minima in the plane of the QW. To release the stored light, we switched off the lateral potential modulation, which resulted in a flat band condition as in the unperturbed case. Attracted by their Coulomb interaction, the electrons and holes approached each other and hence increased the overlap of their wave functions dramatically. The result was an intense flash of luminescence light shortly after the potential modulation was switched off.

This storage mechanism relies on the elec-

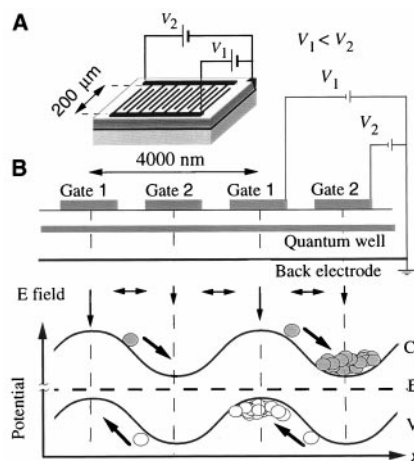


Fig. 1. (A) The optical memory cell, consisting of a semiconductor QW with two interdigitated metal gate electrodes on the surface. (B) Schematic cross section of the storage cell and the lateral electrostatic potential modulation in the plane of the QW caused by the applied gate voltages V_1 and V_2 . Photogenerated e^-h^+ pairs were spatially separated and stored in the modulated potential as indicated. The positions of the conduction band edge (C_B), the Fermi level (E_F), the valence band edge (V_B), and the dominant components of the electric field (E field) are also indicated.

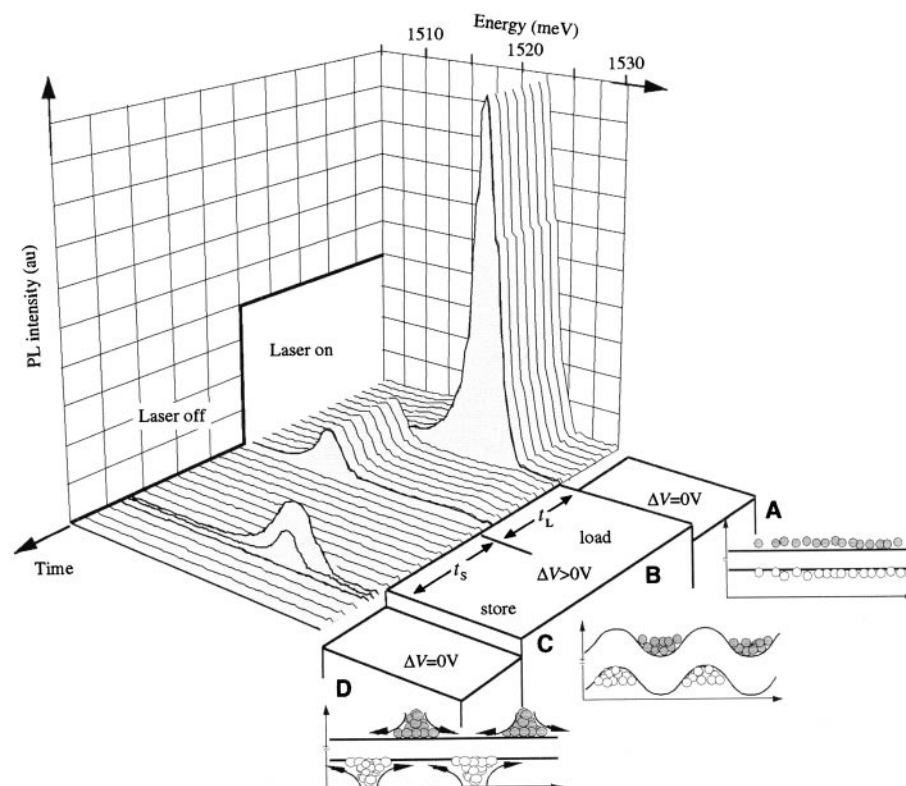


Fig. 2. Photoluminescence spectroscopy verified the storage of photonic signals in the optical memory cell. The graph displays spectra at different experimental conditions and times. Laser and gate voltages were switched as indicated on the time axis. (A) Without potential modulation ($V_1 = V_2 = 0$ V; $\Delta V = 0$ V), a single narrow PL line of photogenerated excitons was observed. (B) The application of small voltages ($V_1 = -0.4$ V and $V_2 = +0.6$ V; $\Delta V > 0$ V); spatially separated electrons and holes in the lateral potential superlattice as indicated. (C) When the laser was switched off, no luminescence could be detected, and electrons and holes remained stored. (D) By resetting the gate voltage modulation to zero ($V_1 = V_2 = 0$ V; $\Delta V = 0$ V), a strong luminescence signal was observed from the recombination of the stored electrons and holes. au, arbitrary units.

trons and holes being separately confined in the plane of a QW and is, in principle, independent of the choice of semiconductor materials. In our experiment, we used a direct band gap GaAs-based QW that was grown by molecular beam epitaxy; the layered structure consisted of a Si-doped back electrode (donor density $N_D = 4 \times 10^{18} \text{ cm}^{-3}$) that was grown on an undoped GaAs buffer and a 20-nm-wide undoped QW that was sandwiched between two short-period AlAs-GaAs superlattice barriers. The QW and the back electrode were separated from the surface by distances of $d_{\text{QW}} = 60 \text{ nm}$ and $d_{\text{BE}} = 390 \text{ nm}$, respectively. On top of the sample surface, we deposited a 10-nm-thick, semitransparent interdigitated Ti gate electrode of periodicity $a = 4000 \text{ nm}$. The width of the individual metal stripes was $w = 1100 \text{ nm}$, and the total gate electrode covered an area of $A = 200 \mu\text{m}$ by $200 \mu\text{m}$. Both the total potential with respect to the back electrode and the amplitude of the lateral potential modulation could be controlled independently. In optimized samples, lateral modulations that are even larger than the effective band gap should be achievable. The resulting structure then would resemble a nipi (n-type/intrinsic/p-type/intrinsic) doping superlattice (8). In contrast, however, our superlattice was not created by a permanent doping modulation but rather by an easily tunable lateral potential modulation.

In the above geometry and with low voltages applied to the gates, we generated strong electric fields of up to 10^5 V/cm , containing both vertical and lateral components. The vertical electric field components were strongest in areas underneath the gate electrodes and influenced the optical properties of the QW through the quantum-confined Stark effect (QCSE) (9). The lateral electric field components that are strongest in areas between the gate electrodes were responsible for the spatial separation of the e^- and h^+

states. For the comparatively large geometry and typical gate bias used, the wave function overlap between the spatially separated e^- and h^+ states was essentially zero.

The sample, stored at temperature $T \approx 100 \text{ K}$ was illuminated by a pulsed laser diode of pulse power $P = 165 \mu\text{W}$ at a wavelength of $\lambda = 820 \text{ nm}$ (1.58 eV) (that is, below the band gap energy of the QW barrier material), resulting in the generation of e^-h^+ pairs in the QW. The light was focused on the gate with a spot size of $\sim 100 \mu\text{m}$ in diameter. The luminescence from the sample was analyzed with a monochromator and a gated photomultiplier. The PL spectra from the sample for different experimental conditions at various discrete times were plotted (Fig. 2, A through D) with the corresponding lateral potential modulation. The gate voltages were chosen so that the Fermi level remained in the effective band gap; that is, we did not have free carriers in either band without illumination.

During the first step of the experiment (Fig. 2A), no bias difference was applied to the gates (voltage $V_1 = V_2 = 0 \text{ V}$; voltage difference $\Delta V = 0 \text{ V}$), and the sample was illuminated with the laser. The interdigitated gate behaved like a homogenous electrode, and the PL from the sample at an energy of about 1.5225 eV was the “usual” spatially direct PL line of a QW with a flat lateral band structure (10). At the given reduced sample temperature of $T = 100 \text{ K}$, this PL line was narrow and intense, which is typical for its excitonic origin. During the next time interval (Fig. 2B), a gate bias difference was applied to the gates ($V_1 = -0.4 \text{ V}$ and $V_2 = +0.6 \text{ V}$; $\Delta V = 1 \text{ V}$) while the sample was illuminated with the laser. Under this condition, the lateral potential modulation resulted in a well-resolved splitting of the PL into two lines (one at 1.515 eV and a weaker line at 1.5227 eV). This splitting and the relative intensities of the lines are characteristic for the induced strong lateral potential modulation, which is caused by the local QCSE underneath the individual gate stripes (10–12). Their intensity ratio indicates exciton transport to areas underneath the stripes, where the QCSE is strongest and the exci-

tonic energies are minimal. The strong overall decrease of the PL intensity was caused by the spatial separation of the e^-h^+ pairs (Fig. 2B). The time interval (Fig. 2B) during which the potential modulation and the laser were “on” simultaneously was referred to as the “loading time” t_L because the minima of the lateral potential modulation were filled with electrons and holes.

The laser was then switched off (Fig. 2C), whereas the potential modulation was kept on. During this “storing time” t_S , no PL was observed. The duration of t_S can be chosen at will and was varied between typical durations of $1 \mu\text{s}$ (as in Fig. 2) and $35 \mu\text{s}$. This period is $\sim 10^4$ times longer than the radiative lifetime of excitons in an unmodulated QW. During t_S , the photogenerated electrons and holes were spatially separated by about one-half of the modulation period and trapped in the lateral potential wells of the conduction and valence bands, respectively. PL was suppressed, as the wave function overlap in this case was negligible. The end of t_S was defined by the instant at which the lateral potential modulation was turned off ($V_1 = V_2 = 0 \text{ V}$; $\Delta V = 0 \text{ V}$). Because they were free to move under their mutual Coulomb attraction, the electrons and holes radiatively recombined, and a bright flash of luminescence light was observed coming from the sample (Fig. 2D), documenting the accumulation of electrons and holes during the loading interval (Fig. 2B) and their long-term storage (Fig. 2C). Because the energetic position of the luminescence flash (Fig. 2D) was identical with the position of the original PL lights in Fig. 2A, we conclude that the recombination of the stored charges was excitonic and originated from the spatially direct transition of a QW with homogeneous lateral bands, as defined by the choice of gate voltages. A proper choice of the total potential applied to the gates can be used to determine the wavelength of the delayed light (10, 12).

A time-resolved measurement of the intensity of the flash in Fig. 2D is shown in Fig. 3. The storage time in this case was $t_S = 17 \mu\text{s}$. The duration of the flash was shorter than the limit of our time resolution (20 ns), but we suppose, however, that the recombination time was much faster according to its excitonic nature. Our experiment showed that low-intensity photonic signals can be accumulated into the structure over long times and then be released at once in a bright short flash. The intensity of this flash as a function of the storage time t_S is shown in Fig. 4. Even for the present unoptimized sample design, very long storage times can be achieved. We restricted ourselves to measurements of times up to $35 \mu\text{s}$, where the detected signal was still well above the noise level, but we anticipate the feasibility of storage times that are

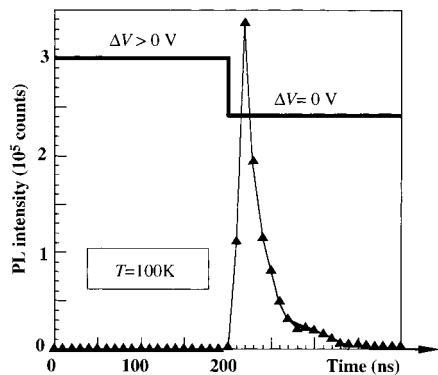


Fig. 3. Time-resolved luminescence signal after a storage time of $t_S = 17 \mu\text{s}$. Resetting the gate voltage difference to zero ($\Delta V = 0 \text{ V}$) triggered an intense flash of light that left the cell within nanoseconds.

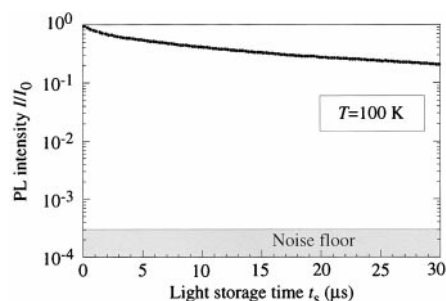


Fig. 4. Time-delayed luminescence intensity I/I_0 (intensity of the PL at $t_S = 0$) for different t_S reflecting storage times in excess of $100 \mu\text{s}$.

>100 μs . The slight decrease of the flash intensity with increasing storage time is thought to be caused predominantly by non-radiative recombination of the stored charges, such as electron tunneling to the gate electrodes. Comparing the intensities of the direct PL (Fig. 2A) with the time-delayed luminescence of Fig. 2D already yields a 12% recovery of the signal for a storage time of 1 μs . The loading time in our experiments was typically $t_L = 3 \mu\text{s}$ at a pulse intensity of $P = 164 \mu\text{W}$. For a longer t_L , the detected flash intensity tended to saturate because eventually the stored electrons and holes screened the lateral potential modulation. We estimate that the maximum charge densities obtained in our device were of the order of 10^{11} per square centimeter.

The storage of photonic signals by the

above means is not restricted to the energy range and material combination that we chose. Different material combinations and sample designs (for example, the use of microcavities) are waiting to be explored. The storage cell presented here works well at temperatures of 100 K. At higher temperatures, the excitons were thermally dissociated as the thermal energy exceeded the exciton binding energy. Then, the PL signals of our present sample became quite weak and spectrally broad. However, newly designed and optimized structures promise room-temperature operation in the near future.

References and Notes

1. C. Gmachl *et al.*, *Science* **280**, 1556 (1998).
2. B. Mukherjee, *Optical Communication Networks* (McGraw-Hill, New York, 1997).

3. D. S. Wiersma, P. Bartolini, A. Lagendijk, *Nature* **390**, 671 (1997).
4. M. Welker *et al.*, *Appl. Phys. Lett.* **71**, 3561 (1997).
5. J. Feldmann *et al.*, *Phys. Rev. Lett.* **59**, 2337 (1987).
6. C. Rocke *et al.*, *ibid.* **78**, 4099 (1997).
7. M. Rufenacht, S. Tsujino, Y. Ohno, *Appl. Phys. Lett.* **70**, 9 (1997).
8. G. H. Döhler *et al.*, *Phys. Rev. Lett.* **47**, 864 (1981).
9. D. A. B. Miller *et al.*, *Phys. Rev. B* **32**, 1043 (1985).
10. A. Schmeller *et al.*, *The Physics of Semiconductors*, D. J. Lockwood, Ed. (World Scientific, Singapore, 1995), pp. 1727–1730; see also A. Schmeller *et al.*, *Appl. Phys. Lett.* **64**, 330 (1994).
11. S. Zimmermann *et al.*, *Phys. Rev. B* **56**, 13414 (1997).
12. S. Zimmermann *et al.*, *Appl. Phys. Lett.* **73**, 154 (1998).
13. We gratefully acknowledge the very useful and enlightening discussions with A. O. Govorov, C. Rocke, and W. Hansen. This work has been sponsored in part by Sonderforschungsbereich 348 of the Deutsche Forschungsgemeinschaft and in part by the Bayerische Forschungsförderung FOROPTO.

16 October 1998; accepted 20 January 1999

Crack Arrest and Multiple Cracking in Glass Through the Use of Designed Residual Stress Profiles

D. J. Green,^{1*} R. Tandon,² V. M. Sglavo³

A processing approach has been identified and reduced to practice in which a residual stress profile can be designed such that cracks in a brittle material are arrested or grow in a stable manner. In the approach, cracks in the body encounter an increase in the magnitude of residual compression as the crack propagates. If correctly designed, the process increases strength and significantly decreases strength variability. This approach was demonstrated for a silicate glass, and multiple cracking was observed as a forewarning of the final failure. Normally, such glasses would fail catastrophically with the propagation of a dominant crack.

Brittle materials, such as ceramics and inorganic glasses, are sensitive to surface contact damage, which gives rise to flaws that reduce strength. Moreover, these materials usually fail in an unstable and catastrophic manner when subjected to applied mechanical and thermal stresses. For example, when most ceramics and glasses are tested in bending, uniaxial tension, or other types of tensile stress fields, a single flaw forms into a propagating crack that grows rapidly and in an unstable manner. The strength behavior is usually modeled with weakest link statistics, such as Weibull statistics, leading to a dependence of strength on specimen size (I). Ex-

tensive damage may also occur in a thermal shock type of loading, resulting in a multiplicity of cracks. In many cases, the crack also branches, forming splinters. This behavior leads to dangers when these materials fail, because there is often no forewarning and the splinters can cause harm. It would be beneficial to develop methods that could stabilize growth or arrest cracks in brittle materials.

Recently, it was shown that the microstructure of some brittle polycrystalline ceramics can be modified such that cracks encounter an increase in fracture resistance as the crack propagates (“rising R curve behavior”), usually by adding fibers, single-crystal whiskers, or transforming particles to the material (I , 2). Crack growth in these materials can be stabilized or cracks arrested even in destabilizing applied stress fields. (A destabilizing field can be defined as one in which the strain energy release rate increases with crack length.) This feature leads to flaw tolerance in the material, wherein the strength

becomes a weak function of crack length. Such cases result in a reduction in strength variability, but in many practical cases also to a reduction in the average strength.

Another approach to improving the mechanical reliability of brittle materials is to find ways to increase their strength. Residual surface compression improves the contact damage resistance and strength of many brittle materials, and various processing techniques are available to introduce such stresses. For example, silicate glasses are often thermally or chemically tempered. Lower expansion coatings, such as glazes, can be applied to ceramics to place the surface into residual compression. An attractive feature of surface compression is that it often leads to a minimum strength value. A limitation of this approach, however, is that failure is still catastrophic under tensile loading conditions. Another widely unrecognized feature of this approach is that an increase in the strength variability may result. In a study on the ion exchange strengthening of silicate glass, the coefficient of variation in the strength increased by almost a factor of 2 for a sixfold strength increase (3). Increased variability leads to difficulties during the design process and is an obstacle to the engineering use of these materials. For brittle materials, design engineers often need to ensure the mechanical reliability in terms of very small failure probabilities at a prescribed design stress level for a given lifetime. In many cases, these levels of failure probability are not easily accessible by experiment alone, leading to the need for statistical and micromechanical modeling. Clearly, it is advantageous to identify processes that can be used to increase strength and decrease strength variability, especially if this affects the behavior at low levels of failure probability.

A solution to the problems outlined above was put forward by Tandon and Green (4–

¹Department of Materials Science and Engineering, Pennsylvania State University, University Park, PA 16802, USA. ²Caterpillar Inc. Technical Center, Peoria, IL 61656, USA. ³Dipartimento di Ingegneria dei Materiali, Università di Trento, I-38050 Trento, Italy.

*To whom correspondence should be addressed. E-mail: green@ems.psu.edu